Volume and Enthalpy Changes in the Early Steps of Bacteriorhodopsin Photocycle Studied by Time-Resolved Photoacoustics

D. Zhang and D. Mauzerall
The Rockefeller University, New York, New York 10021 USA

ABSTRACT We have studied the photoinduced volume changes, energetics, and kinetics in the early steps of the bacteriorhodopsin (BR) photocycle with pulsed, time-resolved photoacoustics. Our data show that there are two volume changes. The fast volume change (≤200 ns) is an expansion (2.5 ± 0.3 Å^3/molecule) and is observed exclusively in the purple membrane (PM), vanishing in the 3-[(3-cholamidopropyl)-dimethylammonio]-1-propane-sulfonate-solubilized BR sample; the slow change (~1 μs) is a volume contraction (−3.7 ± 0.3 Å^3/molecule). The fast expansion is assigned to the restructuring of the aggregated BR in the PM, and the 1-μs contraction to the change in hydrogen bonding of water at Asp 212 (Kandori et al. 1995. *J. Am. Chem. Soc.* 117:2118–2119). The formation of the K intermediate releases most of the absorbed energy as heat, with $\Delta H_K = -36 \pm 8$ kJ/mol. The activation energy of the K → L step is 49 ± 6 kJ/mol, but the enthalpy change is small, −4 ± 10 kJ/mol. On the time scale we studied, the primary photochemical kinetics, enthalpy, and volume changes are not affected by substituting the solvent D_2O for H_2O. Comparing data on monomeric and aggregated BR, we conclude that the functional unit for the photocycle is the BR monomer, because both the kinetics (rate constant and activation energy) and the enthalpy changes are independent of its aggregation state.

INTRODUCTION

Bacteriorhodopsin (BR), the intrinsic membrane protein of *Halobacterium halobium*, converts light energy into electrochemical energy in the form of a proton gradient across the cell membrane (Stoeckenius et al., 1979). The molecular processes of this comparatively simple light energy converter are important, because it is the primal example of a molecular machine. In addition to its role as a light-driven proton pump, BR manifests a rich array of optical and electrical properties. Recently, large efforts have been directed at the study of BR as a biosensor, a photogating device, and an optical information-processing and storage medium (Rees et al., 1994; Hong, 1994; Hampp et al., 1992).

As the only protein in the purple membrane (PM) that forms part of the surface membrane of *Halobacterium halobium*, BR constitutes 75% of the mass of the purple membrane patches; the remainder consists of lipids, mainly phospholipids with ether-linked phytanyl chains. From light scattering experiments (Kubota et al., 1985) it was found that the purple membrane suspended in solution exists in the form of a sheet with a thickness of ~5 nm and a diameter of ~0.5 μm. In these patches, the BR monomer is immobilized as trimers in a two-dimensional hexagonal lattice, presumably by protein-protein interaction (Henderson and Unwin, 1975). Although the natural state of BR is the trimer aggregate, it has been elucidated that the BR monomer is the essential transport unit of this light-driven proton pump (Dencher et al., 1983; Grzesiek and Dencher, 1988). The functional group of this light-energy converter is the retinal chromophore, which is covalently bound through a Schiff base to a lysine residue of the protein moiety. Upon photoexcitation, BR goes through a cyclic series of spectroscopically determined intermediates, as shown in Fig. 1 (Trissl, 1990). Accompanying this process, protons are translocated from the inside (cytoplasmic side) to the outside (exoplasmic side) of the cell membrane, and the light energy is converted into electrochemical energy. This energy is finally stored as ATP formed from the proton gradient across the cell membrane by the much more complex ATPase. BR protein provides a relatively simple system for investigating primary events of an ion pump.

Despite the extensive work on BR, the molecular and kinetic details of the light-driven proton-pumping process are far from fully understood. The measurements of optical absorbance changes have dominated the field, and the ever increasing detail has led to a variety of models (Varo and Lanyi, 1995; Oesterhelt and Tittor, 1989). The use of electrical measurements (Keszthelyi and Ormos, 1980) and of time-resolved infrared measurements (Siebert and Mantele, 1983) has allowed non-retinal-connected events to be determined. Yet much controversy remains. For the simple volume change associated with the K to L step, totally different results have been published. Schulenberg et al. (1995) reported an expansion of 60 cm^3/mol, whereas Varo and Lanyi (1995) observed a volume contraction of much smaller magnitude. The development of the time-resolved photoacoustic (PA) technique provided a powerful tool for studying complicated but previously characterized biosystems (Braslavsky and Heibel, 1992). It has the unique ability to measure enthalpy and volume changes of transient reactions in photochemical processes. It also yields time constants of these reactions and identifies them with steps determined by other spectroscopic methods (Feitelson and Mauzerall, 1993, 1996). Using this technique, we have studied the early transformations in the photocycle of BR,

Received for publication 13 February 1996 and in final form 27 March 1996.

Address reprint requests to Dr. David C. Mauzerall, The Rockefeller University, 1230 York Avenue, New York, NY 10021. Tel.: 212-327-8218; Fax: 212-327-8853; E-mail: mauzera@rockvax.rockefeller.edu.

0006-3495/96/07/381/08 $2.00

Photocycle of Bacteriorhodopsin (BR):

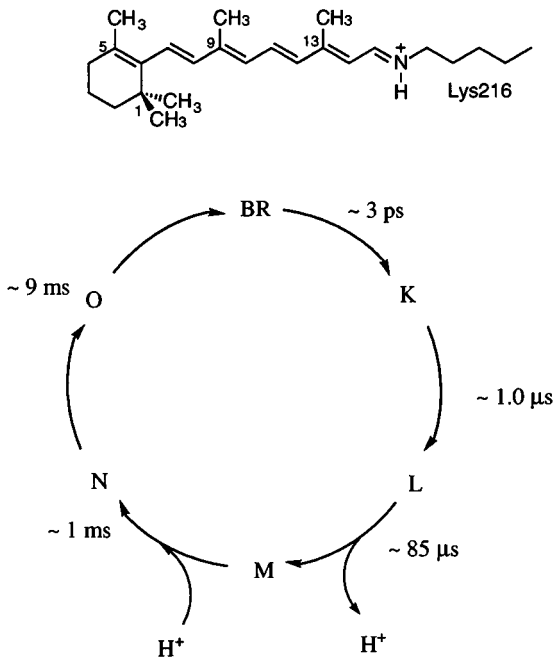

FIGURE 1 The structure of the retinal chromophore of BR in its all-*trans* configuration and the photocycle of light-adapted bacteriorhodopsin. The intermediates are characterized as K, L, M, N, O. The retinal group is covalently bound via the protonated Schiff base to a lysine residue on the protein backbone.

providing important information to clarify the controversy regarding the photoinduced volume changes, energetics, and kinetics. To elucidate the function of BR itself and the role of protein-protein and protein-lipid interactions on its function, we have studied BR, both in its aggregated form of PM and in its monomeric state, when it is solubilized and dissociated in a detergent. Comparing the results of monomeric and aggregated BR and their properties in different environments has led to a better understanding of the proton pump process. Information of this type could provide clues regarding the mechanism of proton translocation and energy transduction, and hence contribute to the field of bioengineering.

MATERIALS AND METHODS

Sample preparation

There were three kinds of BR samples studied in our experiments: the purple membrane in water and in deuterated water and the detergent-solubilized BR. *Halobacterium halobium* was grown, and purple membrane patches containing BR were isolated according to literature protocols (Oesterhelt and Stoeckenius, 1974). The PM/H_2O sample is a suspension of purple membrane fragments in double-distilled water, which was buffered at pH 7 by 10 mM Tris. The absorbance of the sample was adjusted to ~2 at 532 nm in a 1-cm quartz cuvette, corresponding to ~40 μM BR. The PM/D_2O sample was prepared in a similar way by suspending the PM fragments in D_2O buffer solution. To make the detergent-solubilized BR sample, CHAPS (3-[(3-cholamidopropyl)-dimethylammonio]-1-propanesulfonate) was added to the purple membrane water solution. The CHAPS concentration was 15 mM. After sonicating for 30 min (125 W), the solution was centrifuged for 5 min at 15,000 × *g*. The supernatant was characterized by its absorption spectrum before the photoacoustic experiment. All of the BR samples were prepared fresh just before the optoacoustic measurements and were light adapted. For each photoacoustic experiment, the calorimetric reference (Sheaffer black ink), matched in absorbance at 532 nm to that of the BR samples, was measured in the same medium as the sample to calibrate the experimental system and provide the impulse response for the signal convolution. Preliminary measurements proved that this ink was stable with time and light, and gave a response quantitatively identical to those of compounds that degrade absorbed photons to heat on the subnanosecond time scale, e.g., amido black, indigo tetrasulfonate, and congo red.

Photoacoustic experiments

Currently there is some confusion in the literature (Rhor et al., 1992) that a short (picosecond) flash is necessary to avoid exciting intermediates formed by primary photochemistry, e.g., K in the BR cycle. In fact, the probability of such double excitations depends primarily on the photon flux and the optical cross sections of the relevant species. Because for PA experiments one wishes only a single excitation to the initial material, one can use a simple analysis as a starting point. For homogeneous illumination (constant areal light flux, optically thin sample) the excitations will be Poisson distributed (Ley and Mauzerall, 1982; Mauzerall, 1982). The average excitation, X, is σE, where σ is the optical cross section for the light absorption, and E is the flux (photons/area), and the probability of the specific excitation n will be $P_n = X^n \exp(-X)/n!$. Note that at $X = 1$, roughly one-third of the reactants are missed, one-third are hit once, and one-third are excited two or more times. To avoid multiple excitations, one should remain in the region $X = \sigma E < 0.1$. For a common molecular transition ($\sigma = 1$ Å^2, $\epsilon = 3 \times 10^4$ M^{-1} cm^{-1}), this corresponds to 400 μJ/cm^2 at 532 nm. A fully allowed transition may require ten times less flux. The fraction of reactants excited twice or more is

$$P_{\geq 2} = 1 - e^{-x} - Xe^{-x}. \quad (1)$$

The concentration of the pigment, or the ratio of the pigment to photons, often used as a criterion of multiple excitations, is immaterial as long as the sample is optically thin. If the sample is optically thick, this estimate is the safe criterion, because part of the sample will only see a smaller photon flux. If the products formed during the flux time have smaller σ's than the initial reactant, the above criterion is again the correct limit. Only if the product cross section is larger than the reactant does its time of formation matter. If the product is formed instantaneously, i.e., faster than the photon excitation rate, the product molecules excited one or more times are

$$P_{\geq 1} = (1 - e^{-X1})(1 - e^{-X2}), \quad (2)$$

where $X_1 = \phi \sigma_R E$, $X_2 = \sigma_P E$, and ϕ is the yield of R* → P. If $\sigma_P \gg \sigma_R$, then

$$P_{\geq 1} = (1 - e^{-X1}), \quad (3)$$

i.e., a hit to the reactant guarantees a hit to the product. This extreme case has been seen for porphyrins (Ballard and Mauzerall, 1980). If the formation time of the product overlaps the photon excitation rate, the appropriate convolution must be calculated. Marinetti has calculated the case of BR-K-L for long flashes (Marinetti, 1988). We reiterate that the limiting probability of exciting a product is determined by optical cross sections and photon flux, not by absorbance of a sample or the length of the light pulse.

The time-resolved photoacoustic measurements were performed by passing a laser beam through a thermostated solution cell of design similar to that of Arnaut (Arnaut et al., 1992). The temperature of the cell was kept constant within ±0.1°C by circulating thermally controlled water. The laser beam at 532 nm was generated from a "Surelite" (Continuum, TM) Nd-YAG laser with a 7-ns pulse width. The repetition rate was set at 2 Hz to ensure the full

relaxation of BR after each flash, even at the lower temperature. The illuminated area is ~1 cm^2, and the flux energy is ~50 μJ/pulse, which is far below the flux for multiple excitations ($P_{>1} < 1\%$). The acoustic detector is homemade and has been described before (Feitelson and Mauzerall, 1993). Briefly, it consists of a piezoelectric polyvinylidene difluoride film (Kynar, 28-μm thickness) sandwiched between a stainless steel outer jacket (ground) and an inner plunger leading coaxially to a high-impedance, low-noise, nanosecond preamplifier (Amptek 250). The signal is then filtered and further amplified (SRI 560) before being digitized (Tektronix RTD710) and stored in a computer (HP 340) for analysis. The pulse energy of the laser was continuously monitored during the experiment with a joulemeter (J3-09 and JD-2000; Molectron) which sends the digitized signal directly to the computer to normalize the measured signal to constant laser output. Typically, 128 laser shots were averaged, but sometimes 320 shots were used to obtain a better signal-to-noise ratio when the signal was small.

Data analysis

The photoacoustic method is sensitive to volume changes generated by both heat release (Q) and molecular volume changes (ΔV) induced by irradiation. For an instantaneous degradation of the absorbed photons to heat, a pressure change is produced within the system and can be expressed as (Feitelson and Mauzerall, 1993)

$$\delta P = \delta E_a \cdot B \cdot g, \tag{4}$$

where E_a is the light energy absorbed, B is the instrumental constant, containing the compressibility of the medium, and g (= $(\beta/C_p\rho)$) converts heat to volume and is determined by the volume expansivity, β, of the solution, its density, ρ, and its heat capacity, C_p. The actual measured signal evolved with time, $S(t)$, is the convolution of δP with the time derivative of the heat release function, $h'(t)$, over all points located at different distances from the detector,

$$S(t) = E_a \cdot B \cdot g \cdot R(t) * h'(t), \tag{5}$$

where $R(t)$ is the detector impulse response function, and the asterisk denotes the convolution integral. For the reference solution of a compound that releases all of the absorbed energy as heat instantaneously, the heat release function, $h_0(t)$, is a step function, and its derivative $h_0'(t)$ is a delta function; thus the photoacoustic signal can be expressed as

$$S_{ref}(t) = E_a \cdot B \cdot g \cdot R(t) * \delta(t) = E_a \cdot B \cdot g \cdot R(t). \tag{6}$$

For the solution of interest, the photoexcited molecule can distribute the absorbed light energy as heat in three time domains: 1) it may release the heat faster than the time resolution of the apparatus, like the reference, and is referred to as fast heat; 2) it may deliver the heat on a measurable time scale; 3) it may store the energy in a long-lived species that is not measured in the experiment. Thus we have

$$\begin{aligned} S_{sample}(t) &= A_f E_a \cdot B \cdot g \cdot R(t) + A_m E_a \cdot B \cdot g \cdot R(t) * h'(t) \\ &\quad + A_s E_a \cdot B \cdot g \cdot 0 \\ &= A_f \cdot S_{ref}(t) + A_m \cdot S_{ref}(t) * h'(t) + A_s \cdot 0, \end{aligned} \tag{7}$$

where A_f is the fraction of heat released immediately (domain one), A_m is the fraction of heat liberated over the measured time span (domain two), and A_s is the fraction of energy stored in the products for a time long compared to the time of the experiment (domain three) and does not, therefore, contribute to the acoustic signal. Nor does the excited state if it loses energy through emission, e.g., fluorescence. In the case of BR fluorescence, the quantum yield (Φ_{fl}^{BR*} and $\Phi_{fl}^{K} < 10^{-3}$) is negligible (Polland et al., 1986). If an intrinsic volume change is associated with the photo process, it will also be reflected in the corresponding A_i according to its time scale. The sum of the fractions equals unity when normalized to $S_{ref}(t)$,

$$A_f + A_m + A_s = 1. \tag{8}$$

The following reactions are considered for the BR in our experiments:

$$BR + h\nu \rightarrow BR^* \rightarrow K + Q_f + \Delta V_f/g. \tag{9}$$

Because the initial excited state of BR to intermediate K is a rapid process, ~3 ps (Polland et al., 1986), which is much faster than the time resolution of the experiments, the energy released in this step can be treated as fast heat Q_f and counted in the fraction A_f in Eq. 7. ΔV_f is the volume change of the reaction and g translates volume to heat.

$$K \rightarrow L + Q_m + \Delta V_m/g. \tag{10}$$

The formation of intermediate L from K is on the microsecond time scale, which falls in the time range measurable by our instrument. Thus the heat, Q_m, liberated in this step and its volume change, ΔV_m, will be reflected as A_m in our acoustic signal. Because the rest of the photocycle has a time constant longer than that of the experiment, it can be summarized as A_s,

$$L \rightarrow BR + Q_s + \Delta V_s/g. \tag{11}$$

For reactions forming a cycle as the above, we have

$$\Sigma Q_i = E_a \tag{12}$$

$$\Sigma \Delta V_i = 0. \tag{13}$$

The photoacoustic data were analyzed by convoluting the instrument response function, $S_{ref}(t)$, with the derivative of the heat release functions, $h'(t)$, by an iterative procedure according to Eq. 7. For a first-order process the heat formation function is the complement of an exponential ($1 - e^{-kt}$), and therefore, $h'(t) = ke^{-kt}$. The whole range of A_f, A_m, and k was explored, and the best fit with the observed signal, $S_{sample}(t)$, at the same temperature as $S_{ref}(t)$ was determined by a search program for the minimum value of the least-square deviation. According to the above reaction scheme, the A_i coefficients are given by (Feitelson and Mauzerall, 1993)

$$A_f = [\eta_K(Q_f + \Delta V_f/g) + (1 - \eta_K)E_a]/E_a \tag{14}$$

$$\begin{aligned} A_m = \{\eta_K[\eta_L(Q_m + \Delta V_m/g) \\ +(1-\eta_L)(E_a - Q_f)]\}/E_a, \end{aligned} \tag{15}$$

where the quantities η_i are the yields of the respective processes.

In a simple case, if the A_i are temperature independent, this indicates that the intrinsic volume change, ΔV_i, is zero according to Eqs. 14 and 15, because $g = \beta/C_p\rho$ is highly temperature dependent. Then, we can directly obtain the enthalpy change of the reaction from A_i.

However, in general, the A_i are temperature dependent. A convenient way to analyze the data without recourse to tabulated values for $g = \beta/C_p\rho$ is to rescale the $A_i(T)$ at a certain temperature T to room temperature by multiplying the $A_i(T)$ by the ratio of the g factors, g_T/g_{room}. As will be shown in the following, this ratio was directly measured in our experiments (Eq. 18). Therefore, this method allows our results to be exempted from the error introduced by the use of tabulated values of β, which usually refer to pure water or solutions not the same as those used in the experiments. The rescaled A_i, e.g., A_f, can be expressed as

$$\begin{aligned} A_f'(T) &= (g_T/g_{room})A_f(T) \\ &= (g_T/g_{room})[\eta_K(Q_f/E_a) + (1 - \eta_K)] \\ &\quad +(1/g_{room})\eta_K(\Delta V_f/E_a). \end{aligned} \tag{16}$$

The amplitude of the photoacoustic signal for a calibration compound can be expressed as (Norris and Peters, 1993)

$$S_{ref} = B(\beta/C_p\rho)E_a = B\, g\, E_a. \tag{17}$$

B changes by only a few percent over the range in which g_T goes from g_{room} to zero and then becomes negative. The ratio of g_T/g_{room} is, then,

equal to the ratio of the acoustic signal of the reference at these two temperatures and was directly measured in the experiments.

$$S_{ref}(T)/S_{ref}(T_{room}) = g_T/g_{room}. \quad (18)$$

The plot of $A_f'(T)$ against the temperature is remarkably linear. The slope is associated with the heat released (Q_f) through the relationship

$$\text{Slope} = \partial A_f'(T)/\partial T = [\eta_K(Q_f/E_a) + (1 - \eta_K)] \cdot [(1/g_{room})(\partial g_T/\partial T)], \quad (19)$$

assuming the yields, heats released, and volume changes of the reaction do not change over this small temperature range (Westrick et al., 1987). The factor of $[(1/g_{room})(\partial g_T/\partial T)]$ is given by the ratio of the slope ($= BE_a(\partial g_T/\partial T)$ of the plot of the S_{ref} versus temperature to the reference signal at room temperature $S_{ref}(= Bg_{room}E_a)$. Then Q_f/E_a can be obtained from Eq. 19. The feature of this analysis is that it uses only measured data and not arbitrary tabulated values. Furthermore, at the magic temperature, T_m, the temperature of maximum density of water solution where $g = 0$, the intrinsic volume change can be obtained,

$$A_f'(T_m) = (1/g_{room})\eta_K(\Delta V_f/E_a). \quad (20)$$

Calculation of ΔV_f requires the value of g at room temperature, but the absolute error is small and can be corrected by comparing S_{ref} in pure water to that of the working solutions.

RESULTS AND DISCUSSION

Amplitude analysis

PM/water sample

Fig. 2 shows an example of the time-dependent optoacoustic signal generated by PM in water solution (pH 7.0) at room temperature (24.7°C) (*curve a*) and photoacoustic spectra for the same BR sample (*curve b*) and the reference (*curve c*) in the same medium as the sample at the magic temperature, T_m = 3.9°C. In the initial data analysis, we could assume that all acoustic waves have the same temporal shape; this is adequate for the process that occurs faster than the time resolution of the experiment (≤ 200 ns). Thus we only consider the magnitude of the photoacoustic signal, taken as the amplitude of the first peak of the acoustic wave. It is seen that the reference signal at 3.9°C is at the noise level, whereas the signal for the BR sample at the same temperature still shows a positive signal, indicating an expansion of the system, i.e., a volume increase. At the magic temperature (3.9°C), signals arising from thermal expansion are expected to vanish because of the null of the thermal expansivity coefficient ($\beta = 0$) of the water solution. This unique property of water allows the direct determination of the photoinduced volume change. An estimation can be made through the relationship (Mauzerall et al., 1995)

$$\Delta Vr = (1/\eta_k)\gamma h\nu\beta/C_p\rho, \quad (21)$$

where γ is the ratio of the photoacoustic signal of the BR sample at T_m (3.9°C) to that of the reference at room temperature (24.7°C); β, C_p, and ρ are the thermal expansivity, the heat capacity, and the density of the solution at room temperature. h and ν are Planck's constant and the frequency of the absorbed light. Our data reveal a volume increase of 2.3 ± 0.3 Å^3/molecule for the purple membrane in water, assuming a quantum yield of 0.65 (Govindjee et al., 1990).

Light saturation of ΔV_r in PM

We have also measured the light energy saturation for the reaction volume change of PM at T_m (3.9°C). Because the thermal volume change is zero at this temperature, one can observe the saturation of the ΔV_r signal when all BRs are photochemically converted (Fig. 3), without interference from the linearly increasing thermal signal. The saturation signal of BR at T_m (3.9°C) reflects a maximum volume change. The specific volume change per BR was then ob-

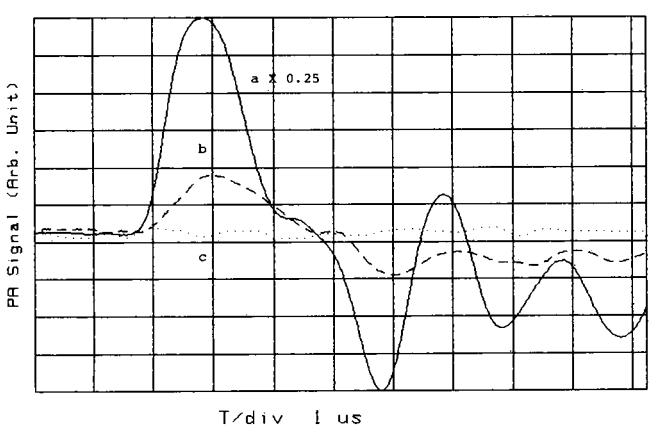

FIGURE 2 The photoacoustic wave (multiplied by 0.25) of the purple membrane in water at room temperature (24.7°C) (*a*) and acoustic waves for the same PM sample (*b*) and for reference (*c*) in the same medium at the magic temperature (3.9°C).

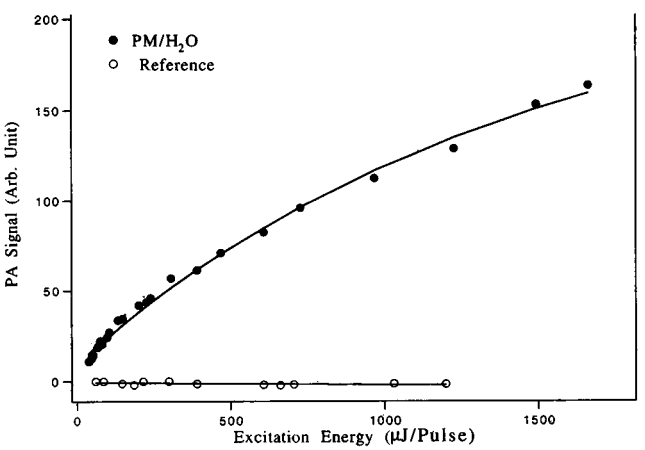

FIGURE 3 Photoacoustic signal of PM in water at 3.9°C, the magic temperature, as a function of the laser excitation energy, E_{exc}. The data were fit to $S = K_0 - K_1 \exp(-\sigma E_{exc})$. This is an approximation to the saturation of molecules with random but fixed orientation during the light pulse (Nagle et al., 1983). However, the difference between the exact curve and the approximation is <10%, and the error in σ is even less. The offset ($K_0 - K_1$) of 5% of the full scale is close to the experimental error.

tained by dividing the maximum volume change by the number of excited BR in the illumination area and found to be 2.4 ± 0.5 Å^3/molecule, which is consistent with the value obtained under the low light flux (see previous section). From the light energy saturation curve, we also calculated the optical cross section of the bacteriorhodopsin as about 1.5 ± 0.3 Å^2/molecule, i.e., $\epsilon = 4 \times 10^4$ M^{-1} cm^{-1}, assuming η_k remains at 0.65. This agrees well with the literature value of $\epsilon = 4.5 \times 10^4$ M^{-1} cm^{-1} at 532 nm (Oesterhelt and Stoeckenius, 1974).

CHAPS-solubilized BR sample

To compare the properties of BR in different states of aggregation, similar experiments were carried out with purple membrane solubilized and dissociated in the CHAPS detergent (CHAPS = 15 mM). In contrast to what we have observed for the purple membrane in water, the photoacoustic signal of the CHAPS-solubilized BR sample is zero at the magic temperature where the reference signal goes to zero. This indicated that there is no photoinduced volume change, $\Delta V_r = 0.2 \pm 0.3$ Å^3/molecule, on the fast time scale when BR molecules are in the monomeric state.

D_2O effect on ΔV_r

To examine the deuterium isotope effect on the reaction, we have performed the photoacoustic measurements on samples of purple membrane in D_2O medium. In addition, the temperature at which the D_2O reaches maximum density and its thermal expansion coefficient goes to zero is ~11°C, which is considerably higher than that of H_2O (3.9°C). Therefore, we have a larger range of temperature to work with between the freezing point and the magic temperature at which the photoacoustic signal becomes negative. In our experiment, the reference signal nulls at 10.8°C in D_2O, reflecting the magic temperature. At this temperature, a positive signal was detected for PM in D_2O, indicating a volume increase, ΔV_r, of 2.5 ± 0.3 Å^3/molecule, which is the same as that of the PM in ordinary water. Comparing results on three kinds of BR samples studied, we found that the volume increase of 2.5 ± 0.3 Å^3/molecule associated with a fast process (≤200 ns) is not affected by the media (H_2O versus D_2O) but changes with the aggregation state. This fast expansion disappears when the PM is solubilized and dissociated by CHAPS, i.e., when BR is in its monomeric state. The restriction of this volume change to the purple membrane leads us to attribute it to the restructuring of the BR trimer cluster, characteristic of the PM (Marinetti, 1988).

Analysis by convolutions

So far, the discussed analysis has assumed that all acoustic waves have the same temporal shape, which is only valid for the process that occurs faster than the time resolution of the experiment (≤200 ns). However, if reactions take place on a time scale that the transducer can resolve (~μs), the result is a significant change in the shape of the photoacoustic wave. Now a more elaborate data analysis is needed to include the consideration of the temporal profile of the acoustic wave. It will also provide detailed thermodynamic and kinetic information covering a larger dynamic range. According to procedures given in the data analysis section, we have performed the convolution of the time derivative of the heat release function with the apparatus response function provided by the reference signal, $S_{ref}(t)$, to fit the acoustic signal, $S_{sample}(t)$, at the same temperature as the reference, using Eq. 7. Series of sets of A_f, A_m, and rate constants at different temperatures and conditions were obtained.

Fast reaction

The fraction of energy released as fast heat, A_f, describes a fast photo process associated with the photoreaction of BR → K. For the PM/water sample, the A_f are temperature dependent. To extract the heat released and the volume change, we have rescaled the A_f according to Eq. 16. The rescaled A_f, A_f', is plotted versus temperature in Fig. 4. From the magnitude of A_f' extrapolated to the magic temperature, $A_f'(T_m)$, a volume increase of $\Delta V_f = 2.6 \pm 0.3$ Å^3/molecule was found from Eq. 20, assuming a quantum yield of $\eta_K = 0.65$ (Govindjee et al., 1990). This is the same as that obtained by the direct measurement at T_m for the PM/water sample (see heading PM/Water Sample, above). To obtain the energy released in this step, we have applied Eq. 19 with the factor of $[(1/g_{room})(\partial g_T/\partial T)]$ obtained from the plot of the reference signal versus temperature, Fig. 4. The quantity Q_f/E_a was found to be 84 ± 4%, corresponding to $\Delta H_K = -36 \pm 8$ kJ/mol for the PM/H_2O sample. This reflects an energy storage of 16% of the 532-nm photon, i.e., ~20% of the $^{BR}E_{00}$ at 613 nm (Birge and Zhang, 1990) in the inter-

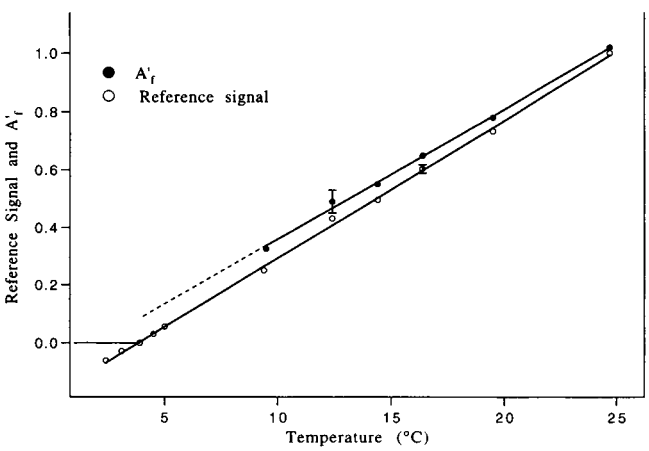

FIGURE 4 The rescaled convolution coefficient A_f' for the PM in water (●) and the amplitude of the photoacoustic signal for the reference (Sheaffer black ink) (○) versus temperature.

mediate K. The same analysis was also performed on data for the other two kinds of samples, the purple membrane in the D_2O medium and the CHAPS-solubilized BR sample. We found that the volume change and the fraction of the absorbed energy released as heat are not affected by the D_2O solvent. They are $\Delta V_f = 2.5 \pm 0.3$ Å^3/molecule and $Q_f/E_a = 85 \pm 4\%$, which are the same as those found for the PM in ordinary water. However, for the CHAPS-solubilized BR sample, although the fraction of the energy released (82 ± 4%) is the same as that for the PM samples, no volume change is discerned from our experiments (0.1 ± 0.3 Å^3/molecule) when the BR molecules are dissociated to their monomeric state. This is in contrast to the volume increase found for the purple membrane in H_2O or D_2O, but is the same result as the direct measurement at T_m (0.2 ± 0.3 Å^3/molecule) for the CHAPS-solubilized BR sample (see above). Thus these two kinds of analysis give consistent results (Table 1). ΔV_f obtained from the convolution has the same magnitude as the previously discussed ΔV_r from the direct measurement and is exclusive to the purple membrane. As before, we attribute this part of the volume change to the structure change of the aggregated BR in the PM. Our data also reveal that the fraction of the energy released in this step is not affected by the aggregation state of BR or the solvent (D_2O versus H_2O). All three BR samples have the same value for the fraction of energy release, ~84 ± 4%, corresponding to the enthalpy change between K and BR, $\Delta H_K = -36 \pm 8$ kJ/mol, which is consistent with the value reported in the literature (Varo and Lanyi, 1991; Birge et al., 1991).

K → L step

Aside from this fast energy-releasing process, convolution analysis reveals that there is another reaction occurring in the measurable time span (microsecond), manifested by the A_m. A similar analysis was performed on A_m to obtain the enthalpy and volume changes on this time scale. We found that there is a volume contraction but very little heat (Table 1) associated with the reaction on this microsecond time scale. The volume change has the same magnitude of −3.7 ± 0.3 Å^3/molecule for all three kinds of samples, regardless of the aggregation state and of the medium (H_2O or D_2O). Because it takes place in the same time range as the lifetime of the K intermediate, ~1.0 μs (Trissl, 1990), we have assigned it to the K to L intermediate transition. This volume contraction might be related to the rearrangement of water bound near the Schiff base. From a Fourier transform infrared (FTIR) study, Kandori et al. (1995) found that on formation of intermediate L, the H-bonding of a water molecule between the Schiff base and Asp 85 becomes stronger and the second originally unbound O-H is now bonded to Asp 212 before the proton transfer. Such formation of an ordered structure is consistent with our finding of some volume decrease from K to L, which was also observed in hydrostatic pressure experiments by Varo and Lanyi (1995). It is noted that all three kinds of samples release most of the light energy absorbed as fast heat, with $\Delta H_K = -36 \pm 8$ kJ/mol. The enthalpy change associated with the transformation of K to L is almost zero, i.e., $\Delta H_{K \rightarrow L} = -4 \pm 10$ kJ/mol (Table 1).

Activation energy of K → L step

The rate constant, k, associated with the K to L transition was also given by the convolution analysis. All three kinds of samples show similar decay lifetime, $\tau = 1/k$, of the K intermediate at corresponding temperatures. A linear relationship between $\ln(k)$ and $1/T$ was observed (Fig. 5). The activation energy was found to be 49 ± 6 kJ/mol from the Arrhenius relationship, which agrees well with the value obtained by spectroscopic method (Varo and Lanyi, 1991; Xie et al., 1987). Again, the activation energy is not affected by the aggregation state or the media. The lack of change of the rate constant of BR on isotopic substitution on the early time is in agreement with electrical measurements (Kono and Ebrey, 1994; Hong, 1992) and is consistent with the finding that the proton transfer occurs later in the photocycle (Trissl, 1990). For the photoreaction of K to L, the rate constants with the values of $\tau = 1/k$ at 25°C and the activation energies are listed in Table 2.

Comparison with other measurements

Our results are inconsistent with the photothermal beam deflection measurements reported by Schulenberg (Schulenberg et al., 1995). They observed a volume contraction of 11 cm^3/mol (18 Å^3/molecule) in the unresolved ≤200-ns time scale and assign it to the BR to K transition in the solution of BR with CHAPS. However, on this time scale (≤200 ns), we did not observe any volume change for BR

TABLE 1 Volume and enthalpy changes for BR samples

	Amplitude analysis	Convolution analysis				
		BR → K		K → L		
Sample	ΔV_r (Å^3/molecule)	ΔV_f (Å^3/molecule)	ΔH_K (kJ/mol)	ΔV_m (Å^3/molecule)	$\Delta H_{K \rightarrow L}$ (kJ/mol)	ΔH_L (kJ/mol)
PM/H_2O	2.3 ± 0.3	2.6 ± 0.3	−36 ± 8	−3.7 ± 0.3	−4 ± 10	−32 ± 10
BR/H_2O (CHAPS = 15mM)	0.2 ± 0.3	0.1 ± 0.3	−40 ± 8	−3.7 ± 0.3	−4 ± 10	−36 ± 10
PM/D_2O	2.5 ± 0.3	2.5 ± 0.3	−34 ± 8	−3.4 ± 0.3	−3 ± 10	−31 ± 10

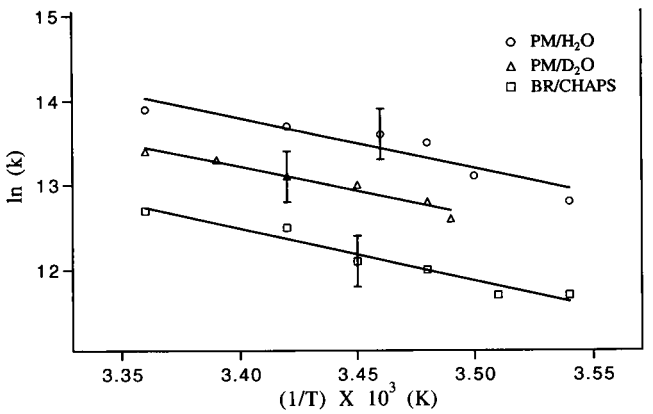

FIGURE 5 Arrhenius plot of the rate constants of photochemical reaction associated with K to L transformation for PM/H_2O (○), PM in D_2O (△) offset by 0.5 unit and CHAPS-solubilized BR sample (CHAPS = 15 mM) (□) offset by 1 unit.

samples with CHAPS of the same concentration. For the purple membrane in water without CHAPS we do detect a volume increase of ~2.5 Å^3/molecule. But this volume change exclusively belongs to the purple membrane and vanishes in samples of PM dissociated by CHAPS. In our case this volume increase was attributed to the rearrangement of aggregated BR in the PM. As for the volume change on the time scale of 1 μs, corresponding to the intermediate K to L transformation, again our results do not agree with those of Schulenberg et al. We detected a photoinduced volume contraction of 3.7 Å^3/molecule, which is much less than the 60 cm^3/mol (~100 Å^3/molecule) expansion observed in their experiments and is of different sign. The difference in magnitude is largely caused by their assumption of a very low quantum yield of 0.09 (Schulenberg et al., 1994). It is known that the overall quantum yield is ~0.65 (Govindjee et al., 1990), so their assumption is unlikely. The major reason for the discrepancy between our data and Schulenberg's is probably their use of a too high photon flux (~10^{16} photons/cm^2) in the ultrashort laser pulse. This leads to multiple excitations of the BR itself, and what they describe as a "steady state" of BR and K. Our light saturation curve (Fig. 3) and calculation of ΔV under these conditions show no indication of this steady-state mixture with large positive ΔV. In contrast to the large volume increase reported by Schulenberg et al., Varo and Lanyi (1995) also found a volume decrease associated with K to L transition with a magnitude much closer to ours (~20 Å^3/molecule). The error associated with their estimation is unstated, but is likely large because of its indirectness, i.e., obtained via pressure effects on the kinetics of the optical cycle. We believe our value of 3.7 Å^3/molecule is reasonable for the volume change caused by the rearrangement of water in the protein matrix, which was observed by FTIR spectroscopy (Kandori et al., 1995).

TABLE 2 Rate constants at 24.7°C and activation energies of K → L step for BR samples

Sample	τ (μs)	E_{act} (kJ/mol)
PM/H_2O	0.9 ± 0.2	49 ± 6
BR/H_2O (CHAPS = 15mM)	1.1 ± 0.2	51 ± 5
PM/D_2O	1.0 ± 0.2	48 ± 5

CONCLUSIONS

We have studied the photoinduced volume changes, energetics, and kinetics associated with the early steps of BR photocycle by time-resolved photoacoustics. There are two volume changes observed for the purple membrane corresponding to different time scales. The volume change occurring on the fast time scale, ≤200 ns, is positive, i.e., a volume increase. This part of the volume change has the same magnitude of 2.5 ± 0.3 Å^3/molecule for the PM in H_2O or D_2O. However, it is sensitive to the aggregation state of BR molecules, vanishing when the PM is dissociated by CHAPS and the BR molecules are in the monomeric state. We have attributed this volume change to the restructuring of the BR trimer cluster in the PM. The volume change occurring on the 1-μs time scale is a contraction (−3.7 ± 0.3 Å^3/molecule). It has the same sign and magnitude for all three kinds of samples, regardless of the aggregation state or the medium (H_2O versus D_2O). We assign this volume change to the K to L intermediate transformation, because it occurs on the same time scale as the lifetime of the K intermediate. It is probably related to the rearrangement of water molecules in the protein matrix, identified by an FTIR study (Kandori et al., 1995). All three kinds of samples release most of absorbed light energy as fast heat on the nanosecond time scale. At the formation of the K intermediate, only ~36 kJ/mol of enthalpy is left for the rest of the photocycle, i.e., ΔH_K = −36 ± 8 kJ/mol, corresponding to an energy storage of ~20% of the $^{BR}E_{00}$ state, which is consistent with that reported in the literature (Birge et al., 1991). The activation energy for the photochemical reaction associated with the K to L step is ~49 ± 6 kJ/mol and is the same for all three samples. On the time scale that we studied, the primary photochemical energy storage, kinetics, and volume changes were not affected by the solvent, H_2O versus D_2O (Kono and Ebrey, 1994). This is consistent with the fact that the proton transfer is not involved until the formation of intermediate M, which occurs over many tens of microseconds. Our data provide further evidence that the functional unit responsible for the BR photocycle is the monomer itself, because both the kinetics (rate constant and activation energy) and the thermodynamics (enthalpy change) are independent of the aggregation state of the BR molecule.

This work was supported by a National Institutes of Health grant, GM 25693.

REFERENCES

Arnaut, L. G., R. A. Caldwell, J. E. Elbert, and L. A. Melton. 1992. Recent advances in photoacoustic calorimetry: theoretical basis and improvements in experimental design. *Rev. Sci. Instrum.* 63:5381–5389.

Ballard, S. G., and D. Mauzerall. 1980. Photochemical ionogenesis in solutions of zinc octacthylporphyrin. *J. Chem. Phys.* 72:933–947.

Birge, R. R., T. M. Cooper, A. F. Lawrence, M. B. Masthay, C. Zhang, and R. Zidovetzki. 1991. Revised assignment of energy storage in the primary photochemical event in Bacteriorhodopsin. *J. Am. Chem. Soc.* 113:4327–4328.

Birge, R. R., and C. F. Zhang. 1990. Two-photon double resonance spectroscopy of bacteriorhodopsin assignment of the electronic and dipolar properties of the low-lying ^{1}Ag*-like and ^{1}Bu*-like π, π* states. *J. Chem. Phys.* 92:7178–7195.

Braslavsky, S. E., and G. E. Heibel. 1992. Time-resolved photothermal and photoacoustic methods applied to photoinduced processes in solution. *Chem. Rev.* 92:1381–1410.

Dencher, N. A., K.-D. Kohl, and M. P. Heyn. 1983. Photochemical cycle and light-dark adaptation of monomeric and aggregated bacteriorhodopsin in various lipid environments. *Biochemistry.* 22:1323–1333.

Feitelson, J., and D. Mauzerall. 1993. Wide-band, time-resolved photoacoustic study of electron-transfer reactions: photoexcited magnesium porphyrin and quinones. *J. Phys. Chem.* 97:8410–8413.

Feitelson, J., and D. Mauzerall. 1996. Photoacoustic evolution of volume and entropy changes in energy and electron transfer. Triplet state porphyrin with oxygen and naphthoquinone-2-sulfonate. *J. Phys. Chem.* 100:7698–7703.

Govindjee, R., S. P. Balashov, and T. G. Ebrey. 1990. Quantum efficiency of the photochemical cycle of bacteriorhodopsin. *Biophys. J.* 58: 597–608.

Grzesiek, S., and N. A. Dencher. 1988. Monomeric and aggregated bacteriorhodopsin: single-turnover proton transport stoichiometry and photochemistry. *Proc. Natl. Acad. Sci. USA.* 85:9509–9513.

Hampp, N., A. Popp, C. Braeuchle, and D. Oesterhelt. 1992. Diffraction efficiency of BR films for holography containing bacteriorhodopsin wildtype BR_{WT} and its variant BR_{D85E} and BR_{D96N}. *J. Phys. Chem.* 96:4679–4685.

Henderson, R., and P. N. T. Unwin. 1975. Three-dimensional model of purple membrane obtained by electron microscopy. *Nature.* 257:28–32.

Hong, F. T. 1992. Bioelectrochemical processes in photobiological membranes. *Biophys. Membr. Transp.* 11:217–242.

Hong, F. T. 1994. Retinal proteins in photovoltaic devices. *Adv. Chem. Ser.* 240:527–59.

Kandori, H., Y. Yamazaki, J. Sasaki, R. Needleman, J. K. Lanyi, and A. Maeda. 1995. Water-mediated proton transfer in proteins: an FTIR study of bacteriorhodopsin. *J. Am. Chem. Soc.* 117:2118–2119.

Keszthelyi, L., and P. Ormos. 1980. Electric signals associated with the photocycle of bacteriorhodopsin. *FEBS Lett.* 109:189193.

Kono, M., and Ebrey, T. G. 1994. The K to L transiton of bacteriorhodopsin does not appear to be controlled by a proton transfer. *Biophys. J.* 66:A45.

Kubota, K., Y. Tominaga, S. Fujime, J. Otomo, and A. Ikegami. 1985. Dynamic light scattering study of suspensions of purple membrane. *Biophys. Chem.* 23:15–29.

Ley, A. C., and D. Mauzerall. 1982. Absolute absorption cross-sections for photosystem II and the minimum quantum requirement for photosynthesis in the *Chlorella vulgaris*. *Biochim. Biophys. Acta.* 680:174–180.

Malkin, S., M. S. Churio, S. Shocjat, and S. E. Braslavsky. 1994. Photochemical energy storage and volume changes in the microsecond time range in bacterial photosynthesis a laser induced optoacoustic study. *J. Photochem. Photobiol. B. Biol.* 23:79–85.

Marinetti, T. 1988. Nonproton ion release by purple membranes exhibits cooperativity as shown by determination of the optical cross-section. *Biophys. J.* 54:197–204.

Mauzerall, D. 1982. Statistical theory of the effect of multiple excitation in photosynthetic systems. *In* Biological events probed by ultrafast laser spectroscopy. R. R. Alfano, editor. Academic Press, New York. 215–235.

Mauzerall, D., M. R. Gunner, and J. W. Zhang. 1995. Volume contraction on photoexcitation of the reaction center from rhodobacler sphaeroides R-26: internal probe of dielectrics. *Biophys. J.* 68:275–280.

Nagle, J. F., S. M. Bhattacharjee, L. A. Parodi, and R. H. Lozier. 1983. Effect of photoselection upon saturation and the dichroic ratio in flash experiments upon effectively immobilized systems. *Photochem. Photobiol.* 38:331–339.

Norris, C. L., and K. S. Peters. 1993. A photoacoustic calorimetry study of horse carboxymyoglobin on the 10-nanosecond time scale. *Biophys. J.* 65:1660–1665.

Oesterhelt, D., and W. Stoeckenius. 1974. Isolation of the cell membrane of *Halobacterium halobium* and its fractionation into red and purple membrane. *Methods Enzymol.* 31A:667–678.

Oesterhelt, D., and J. Tittor. 1989. Two pumps, one principle: light-driven ion transport in Halobacteria. *Trends Biochem. Sci.* 14:57–61.

Polland, H. J., M. A. Franz, W. Zinth, W. Kaiser, and D. Oesterhelt. 1986. Energy transfer from retinal to amino acids—a time-resolved study of the ultraviolet emission of bacteriorhodopsin. *Biochim. Biophys. Acta.* 851:407–415.

Rees, D. C., A. J. Chirino, K. H. Kim, and H. Komiya. 1994. Membrane protein structure and stability: implications of the first crystallographic analyses. *Methods Physiol. Ser.* 1:3–26.

Rhor, M., W. Gartner, G. Schweitzer, A. R. Holzwarth, and S. E. Braslavsky. 1992. Quantum yields of the photochromic equilibrium between Bacteriorhodopsin and its bathointermediate K. Femto- and nanosecond optoacoustic spectroscopy. *J. Phys. Chem.* 96:6055–6061.

Schulenberg, P. J., W. Gartner, and S. E. Braslavsky. 1995. Time-resolved volume changes during the Bacteriorhodopsin photocycle: a photothermal beam deflection study. *J. Phys. Chem.* 99:9617–9624.

Schulenberg, P. J., M. Rohr, W. Gartner, and S. E. Braslavsky. 1994. Photoinduced volume changes associated with the early transformation of bacteriorhodopsin: a laser-induced optoacoustic spectroscopy study. *Biophys. J.* 66:838–843.

Siebert, F., and W. Mantele. 1983. Investigation of the primary photochemistry of Bacteriorhodopsin by low temperature Fourier transform infrared spectroscopy. *Eur. J. Biochem.* 130:565–573.

Stoeckenius, W., R. H. Lozier, and R. A. Bogomolni. 1979. Bacteriorhodopsin and the purple membrane of halobacteria. *Biochim. Biophys. Acta.* 505:215–278.

Trissl, H.-W. 1990. Photoelectric measurements of purple membranes. *Photochem. Photobiol.* 51:793–818.

Varo, G., and K. Lanyi. 1991. Thermodynamics and energy coupling in the bacteriorhodopsin photocycle. *Biochemistry.* 30:5016–5022.

Varo, G., and K. Lanyi. 1995. Effects of hydrostatic pressure on the kinetics reveal a volume increase during the Bacteriorhodopsin photocycle. *Biochemistry.* 34:12161–12169.

Westrick, J. A., J. L. Goodman, and K. S. Peters. 1987. A time-resolved photoacoustic calorimetry study of the dynamics of enthalpy and volume changes produced in the photodissociation of carbon monoxide from sperm whale carboxymyoglobin. *Biochemistry.* 29:6741–6746.

Xie, A. H., J. F. Nagle, and R. H. Lozier. 1987. Flash spectroscopy of purple membrane. *Biophys. J.* 51:627–635.